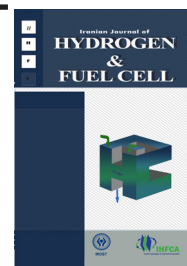


Iranian Journal of Hydrogen & Fuel Cell

IJHFC

Journal homepage://ijhfc.irost.ir



La_{0.6}Sr_{0.4}Co_{0.2}Fe_{0.8}O₃ perovskite cathode for intermediate temperature solid oxide fuel cells: A comparative study

E. Mostafavi, A. Babaei*, A. Ataie

School of Metallurgy and Materials Engineering, College of Engineering, University of Tehran, P.O. Box 14395-553, Tehran, Iran

Article Information

Article History:

Received:

22 June 2015

Received in revised form:

24 August 2015

Accepted:

9 September 2015

Keywords

Perovskites

LSCF

Nanoparticles

Co-precipitation

Cathodes

Solid Oxide Fuel Cells

Abstract

In this study the characteristics of two different kinds of La_{0.6}Sr_{0.4}Co_{0.2}Fe_{0.8}O₃ (LSCF) powders, one in-house powder synthesized by a co-precipitation method and another purchased from the Fuel Cell Materials Co. (FCM Co., USA) were compared. The co-precipitated powder was prepared by using ammonium carbonate as the precipitant with a NH₄⁺/NO₃⁻ molar ratio of 2 and calcination at 1000°C for 1 h. Phase composition, morphology and particle size distribution of powders were systematically studied using X-ray diffraction (XRD), field emission scanning electron microscopy (FESEM) and laser particle size analysis (LPSA), respectively. The synthesized and commercial LSCF powders were overlaid on an Yttria-stabilized zirconia (YSZ) electrolyte having a gadolinium-doped ceria (GDC) interlayer. Electrochemical Impedance Spectroscopy (EIS) measurements were carried out at various operating temperatures in the range of 600-850°C. XRD and FESEM analysis revealed that single phase nano-crystalline LSCF powder with a mean crystallite size of 14 nm and mean particle size of 90 nm was obtained after calcination at 1000°C. The presence of hard agglomerated particles larger than a few microns in the commercial powder and also sub-micron agglomerates in the co-precipitated LSCF powder might be related to the final mechanical milling process and high calcination temperature of powders, respectively. LPSA results showed an identical mean particle size of about 1.5 μm for both LSCF powders. EIS results revealed almost identical polarization resistance for both LSCF powders.

1. Introduction

Fuel cells constitute an attractive power-generation technology that converts chemical energy directly into electrical energy with high efficiency and low emission of pollutants [1]. In particular solid oxide fuel

cells (SOFCs) are important as they can be used with a wide variety of fuels including hydrocarbons and alcohols and are affected less by impurities compared to polymer electrolyte membrane (PEM) fuel cells [2]. However, they suffer from some drawbacks such as a high level of cost and also degradation due to the high

*Corresponding author. Tel.: +98 21 82084607; fax: +98 21 88006076,
E-mail address: alireza.babaei@ut.ac.ir

operating temperature of a SOFC stack. In this regard, most recent studies have been focused on decreasing the operating temperature to an intermediate range of 500-700°C in order to lower the cost and to extend the lifetime of SOFCs [3]. Perovskite-type complex oxides are of great interest in SOFC structure due to their fantastic properties, low cost and varied applications [4]. The ability of perovskite oxide materials to show high ionic and electronic conduction as well as appropriate catalytic activity makes them very promising materials to be used in SOFCs as the main materials for anode and cathode electrodes, interconnector coating and even electrolyte [5, 6].

Cathode materials for SOFC application should possess high electrical conductivity and high electrocatalytic activity for the oxygen reduction reaction as well as sufficient porosity to facilitate the transportation phenomena [6, 7]. Although $\text{La}_{1-x}\text{Sr}_x\text{MnO}_3$ (LSM) perovskite used to be the best choice of cathodes for high temperature SOFCs, nowadays, its application in IT-SOFCs is seriously limited due to its very low ionic conductivity and poor electrocatalytic activity in the lower temperature range [7]. $\text{La}_{1-x}\text{Sr}_x\text{Co}_{1-y}\text{Fe}_y\text{O}_3$ (LSCF), especially the composition of $\text{La}_{0.6}\text{Sr}_{0.4}\text{Co}_{0.2}\text{Fe}_{0.8}\text{O}_3$, as a mixed ionic–electronic conductor (MIEC) is an attractive cathode material for intermediate temperature SOFCs which show high activity, high thermal and chemical stability, high mixed electronic-ionic conductivity and high compatibility with other fuel cell materials. In addition to SOFC cathode material, this compound has multifunctional applications as a catalyst for combustion and oxidative coupling of hydrocarbons and oxygen separation membranes [7-10].

LSCF compounds for SOFC application have been synthesized via different routes such as the conventional solid state method [11], combustion synthesis [12], co-precipitation [10, 11], citrate gel [11, 13] and gel-casting [13]. The co-precipitation method is a simple route to prepare fine, nano-crystalline, high-purity and homogeneous powders of single or multi-component oxides which enable appropriate control of morphology and size of the particles [14]. Extensive research shows that cathode performance

in SOFCs is strongly dependent on the morphology, microstructure and distribution of cathode material particles [15]. There are several different approaches to enhance the electrochemical performance of SOFCs such as using composite electrodes [2, 16] and nanostructured materials [17], lowering the average size of electrode nanoparticles [18], manipulating the particle size distribution of electrode materials [15] and changing the morphology of the particles [2]. It is reported that overlaying a GDC interlayer between the electrode and electrolyte is an effective way to improve the electrochemical performance by preventing the undesired solid state reaction between the YSZ electrolyte and LSCF cathode. Kim et al. [3] found that the GDC interlayer should be sufficiently dense and uniform to prevent the destructive reactions between LSCF and YSZ that may lead to the formation of undesired phases such as SrZrO_3 and $\text{La}_2\text{Zr}_2\text{O}_7$, which significantly deteriorates the cell performance. In this regard, Duan et al. [19] reported severe solid state reactions between YSZ and GDC at 1300 °C, and suggested that 1250 °C is the best sintering temperature for the GDC interlayer. Also, Mai et al. [20] investigated the structural properties of the GDC interlayer and found the best performance with an optimal sintering temperature of 1250 °C to maximize the density of the interlayer while minimizing the formation of a solid solution between GDC and YSZ.

In this study, single phase $\text{La}_{0.6}\text{Sr}_{0.4}\text{Co}_{0.2}\text{Fe}_{0.8}\text{O}_3$ perovskite was successfully synthesized by a simple co-precipitation method. In order to investigate the applicability of the powder synthesized by a simple and low cost co-precipitation method as a SOFC cathode material, the phase composition, microstructure and electrochemical performance of the co-precipitated powder were compared with those of a commercial LSCF powder at the operating temperature range of 600-850 °C.

2. Experimental

$\text{La}_{0.6}\text{Sr}_{0.4}\text{Co}_{0.2}\text{Fe}_{0.8}\text{O}_3$ (LSCF) compound was synthesized by a co-precipitation route using high

purity analytical grade metal nitrates (Merck) and an ammonium carbonate ($\text{CH}_6\text{N}_2\text{O}_2 \cdot \text{CH}_5\text{NO}_3$, Merck) with a $(\text{NH}_4^+/\text{NO}_3^-)$ molar ratio of 2. The details of the synthesis procedure are reported in [21]. Dense YSZ electrolyte substrates were prepared as described in [22]. In order to prevent formation of unwanted compounds between the LSCF and YSZ electrolytes, a thin GDC ($\text{Ce}_{0.9}\text{Gd}_{0.1}\text{O}_2$) interlayer was applied on top of the YSZ electrolyte by a screen printing technique followed by sintering at 1250 °C for 2 h. The cathode layer was prepared by mixing the LSCF powder with an ink vehicle (Fuel Cell Materials Co., USA) and applying it on the GDC interlayer and subsequently sintering at 1050 °C for 2 h.

The phase formation of the synthesized powder was studied by the X-ray diffraction (XRD) technique using a Philips PW-1730 apparatus with Cu K_α radiation ($\lambda=1.5406 \text{ \AA}$) in the range of $20^\circ \leq 2\theta \leq 80^\circ$ and step size of 0.02° . The microstructure of the LSCF powders and fabricated cathodes were observed by a field emission scanning electron microscope (FESEM, TESCAN MIRA3) and scanning electron microscope (SEM, Cambridge S360), respectively. The mean particle size was calculated using MIP (Microstructural Image Processing) software to measure more than 20 particles from the FESEM images. The size distribution of the powders was investigated using the laser particle size analysis (LPSA) method. For comparison of the specifications a commercial LSCF powder with a similar composition, denoted here as LSCF (FCM), was obtained from the Fuel Cell Materials Co. USA.

Electrochemical measurements were carried out using a PARSTAT 2273 potentiostat. A three electrode system comprised of working, counter and reference electrodes was used for the electrochemical measurements. The electrochemical impedance spectra were measured at open circuit potential in the frequency range of 0.1 Hz –100 kHz with a signal amplitude of 10 mV at operating temperatures in the range of 600- 850 °C. All three electrodes were exposed to open air. Pt mesh was used to collect current.

3. Results and discussion

Fig. 1 shows X-ray diffraction patterns of commercial LSCF (FCM) powder along side the co-precipitated powders by ammonium carbonate with a $(\text{NH}_4^+/\text{NO}_3^-)$ molar ratio of 2 and pH of 8.5, after calcination at different temperatures in the range of 900-1100 °C. XRD results revealed that at the calcination temperature of 900 °C a minor secondary phase is present and formation of perovskite phase was not complete, while at the temperature of 1000 °C a single phase crystalline LSCF provskite was formed and we note it herein as LSCF (1000). Further increasing the calcination temperatures up to 1100 °C increased the crystallinity of the powders. Previous reports also showed formation of a pure $\text{La}_{0.6}\text{Sr}_{0.4}\text{Co}_{0.2}\text{Fe}_{0.8}\text{O}_3$ phase at the temperatures in the range of 900-1000 °C [11, 13]. Additionally, mean crystallite size of commercial LSCF (FCM) and synthesized LSCF (1000) powders were calculated from XRD patterns and the values of 19 and 10 nm were obtained, respectively.

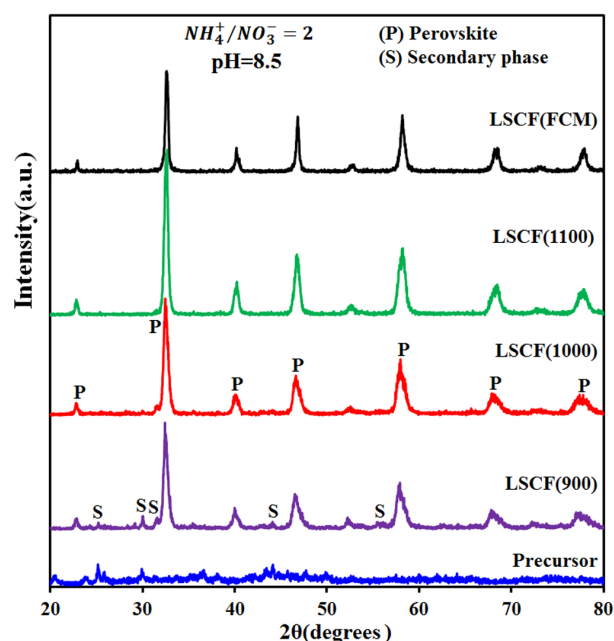


Fig. 1. XRD patterns of the precursor processed by $(\text{NH}_4^+/\text{NO}_3^-)=2$ at pH=8.5 and the commercial FCM powder after calcination at different temperatures in the range of 900-1100 °C.

Fig. 2 shows the FESEM micrographs of LSCF (FCM) and LSCF (1000) powders. The presence of faceted plate-like particles with a wide size distribution in the commercial powder, seen in Fig. 2a, might be due to a final milling process on the powders which makes it difficult to exactly estimate the mean particle size of the powder. On the other hand, hard agglomerated semi-spherical nanoparticles with a mean particle size of 90 nm were observed in the LSCF (1000) powder. Such a hard agglomerated LSCF powder with a mean particle size of 50 nm was also observed by Dutta et al. [12], even at a low calcination temperature of 700 °C. In another research, hard agglomerated LSCF particles with irregular shape were synthesized by the mixed oxide method, while the co-precipitation method leads to the formation of large particles with a highly textured surface. Richardson et al. reported that utilizing a citrate-gel method causes formation of a highly porous morphology [11].

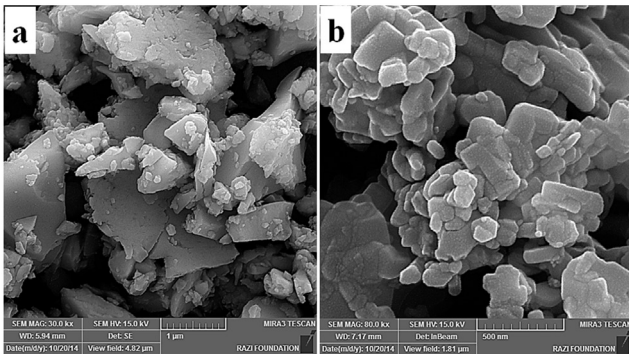


Fig. 2. FESEM micrographs of (a) commercial LSCF (FCM), and (b) LSCF (1000) powders.

Fig. 3 demonstrates the electrochemical impedance spectra (EIS) for the commercial LSCF (FCM) and synthesized LSCF (1000) cathodes under open circuit conditions in an operating temperature range of 650-850 °C. All the ohmic resistances of the EIS spectra were set to 0.1 $\Omega \cdot \text{cm}^2$ for better comparison of the impedance arcs. The obtained polarization resistance data are slightly smaller than those reported by Chen et al [23]. Although the individual particle size of the LSCF (1000) powder was much finer compared to that of LSCF (FCM) powder, the cell

performance data showed almost identical results. As seen in the inset of Fig.3, at 700 °C the LSCF (1000) cathode exhibited almost the same electrochemical response with the cathode fabricated from the LSCF (FCM) powder. Considering the morphology of LSCF particles from Fig. 2, a better performance was expected from the LSCF (1000) cathode rather than the LSCF (FCM) due to the finer particle size of synthesized powder, but no significant difference was observed in the electrochemical response of the electrodes. Therefore, another factor must have an important role in controlling the electrode performance.

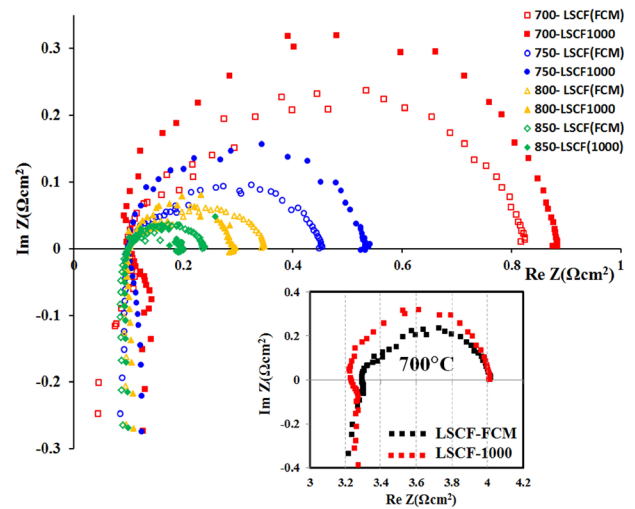


Fig. 3. Electrochemical impedance spectra (EIS) for the LSCF (FCM) and the LSCF (1000) cathodes in an operating temperature range of 700-850 °C.

The reason behind this contradiction could be related to the strong effect of the particle size distribution of electrode materials, which is in a good agreement with the LPSA results of the LSCF powders presented in Fig.4. It is notable that the particle size distribution of the LSCF (FCM) powder was reported in the range of 0.7- 1.1 μm in a data sheet presented by Fuel Cell Materials Co. [24]. Contrary to this, we observed two split peaks in the LPSA diagrams, which could be related to the existence of two groups of particles with different sizes. A group of fine particles was in the range of 0.3-0.6 μm , and another group of hard agglomerated particles in the range of 2-3 μm . As it can be observed, both synthesized and commercial LSCF powders

show the same particle distribution characteristics and a mean particle diameter of $1.5\mu\text{m}$ was reported for both. It is well known that particle size distributions of powders have a significant effect on the sintering behavior, physical and electrochemical performance of the cathode materials [15]. Although both the LSCF powders were previously roll-milled in acetone for 32 h before the LPSA experiment with an aim to increase the homogeneity of the powders, this process was not effective for obtaining a uniform distribution of particle size. Thus, it can be concluded that these powders consist of hard agglomerated particles which even prolonged roll milling could not convert to discrete particles. It is worth mentioning that for co-precipitated LSCF powders, increasing the calcination temperature from 1000 to 1100 °C increased the mean particle size from 1.5 to 90 μm (not shown), which indicates the severe sintering of particles at very high calcination temperatures.

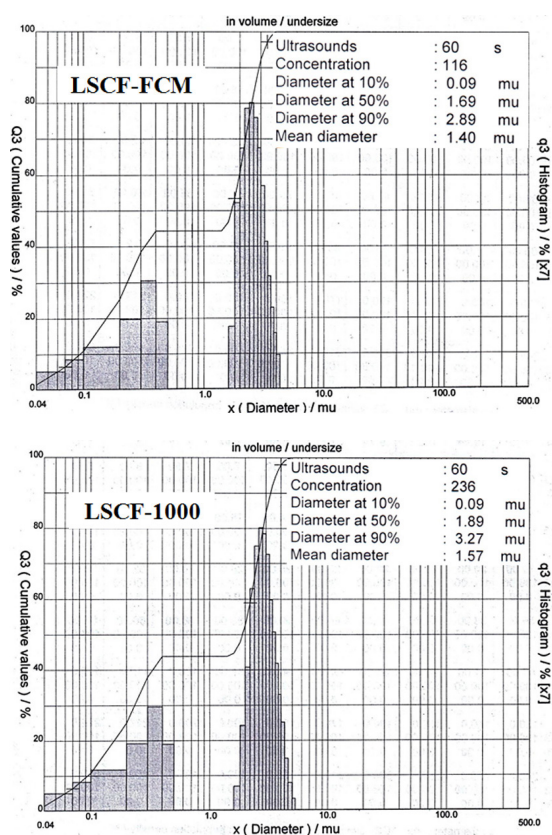


Fig. 4. Particle size distributions of LSCF (FCM) and LSCF (1000) powders.

Fig. 5 shows the SEM micrographs of LSCF half cells. Fig. 5a depicts a comprehensive view of a cathode half-cell which consists of a porous LSCF cathode (top layer), a GDC interlayer (middle layer) and a dense YSZ electrolyte (bottom layer). The porous structure of the LSCF cathode layers is clearly seen in Figs. 5b and 5c. Also, sintering of the LSCF cathodes at 1050 °C for 2 h resulted in a well-necked grains as well as appropriate porosity volume. The mean grain size of the LSCF (FCM) and LSCF (1000) cathode particles was estimated to be 700 and 160 nm, respectively. By comparing these values with the mean particle size of LSCF powders from Fig. 2, it can be concluded that the grains of the LSCF (1000) cathode were retained fairly fine and uniform after sintering at 1050 °C for 2 h. Furthermore, Fig. 5d shows the overall view of the YSZ-GDC-LSCF layers.

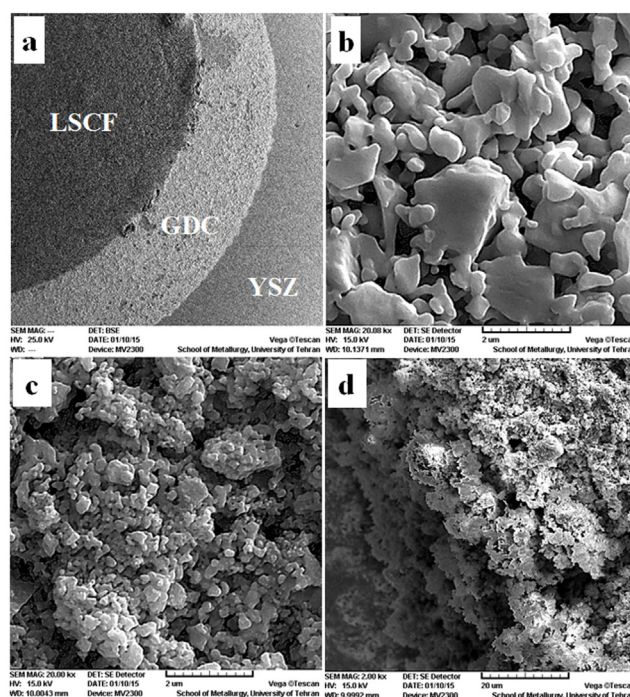


Fig. 5. SEM micrographs of (a) a half cell containing YSZ electrolyte, GDC interlayer and LSCF cathode; the surface of (b) LSCF (FCM) and (c) LSCF (1000) cathode materials both sintered at 1050 °C for 2 h, and (d) overall view of YSZ & GDC & LSCF (1000) layers.

Fig. 6. indicates the temperature dependence of the polarization resistance for synthesized and

commercial LSCF cathodes, sintered at 1050 °C and measured within the range of 600-850 °C. As shown, polarization resistance decreased with increasing temperature. Also, the polarization resistance values were almost identical for both LSCF-based cathodes. Calculated activation energy values for both LSCF cathodes were similar, around 130 kJ/mol, which is fairly small compared to other reports [10, 16, 25, 26].

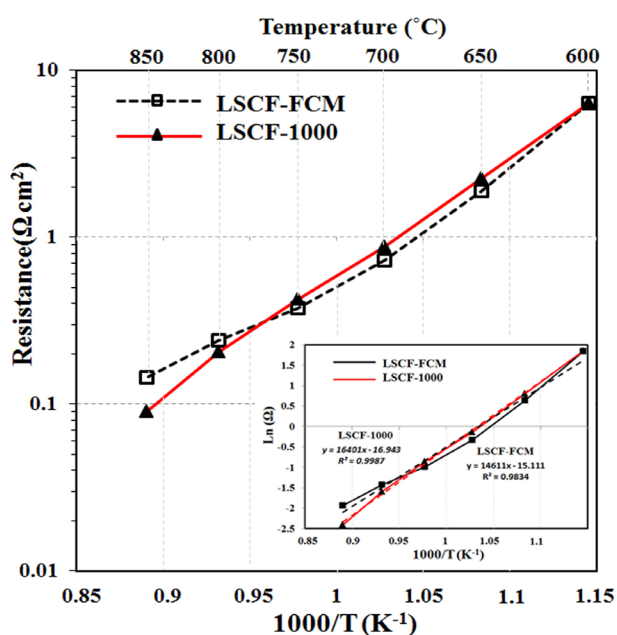


Fig. 6. Temperature dependence of the polarization resistance for LSCF (FCM) and LSCF (1000) cathodes under open circuit conditions measured at various temperatures of 600-850 °C.

4. Conclusions

Nano-crystalline $\text{La}_{0.6}\text{Sr}_{0.4}\text{Co}_{0.2}\text{Fe}_{0.8}\text{O}_3$ powder was successfully synthesized via the co-precipitation method using metal nitrates as starting materials and ammonium carbonate as the precipitant agent. XRD and FESEM analysis revealed that a LSCF powder with a mean crystallite size of 14 nm and mean particle size of 90 nm was obtained after calcination at 1000 °C. EIS measurements were carried out for cathodes fabricated from synthesized and commercial LSCF powders at various operating temperatures in the range of 600-850 °C and revealed almost identical

polarization resistance for both LSCF powders. Polarization resistance of the cathode electrode was measured equal to 0.7 and 0.76 $\Omega\cdot\text{cm}^2$ for LSCF (FCM) and LSCF (1000), respectively. It is concluded that particle size distribution of the LSCF cathode material plays an important role in improvement of the cell performance. An activation energy of around 130 kJ/mol for oxygen reduction reaction was calculated for both LSCF powders.

5. Acknowledgment

The financial support for this work by the University of Tehran under grant number 29920/1/01 is gratefully acknowledged. The support of the Renewable Energy Organization of Iran for this work is also acknowledged.

6. References

- [1] B. C. Steele and A. Heinzel, "Materials for fuel-cell technologies," *Nature*, 2001, 414: 345.
- [2] J. Fergus, R. Hui, X. Li, D. P. Wilkinson, and J. Zhang, *Solid oxide fuel cells: materials properties and performance*: CRC press, 2008.
- [3] W.-H. Kim, H.-S. Song, J. Moon, and H.-W. Lee, "Intermediate temperature solid oxide fuel cell using (La,Sr) (Co,Fe) O_3 based cathodes," *Solid State Ionics*, 2006, 177: 3211.
- [4] M. Pena and J. Fierro, "Chemical structures and performance of perovskite oxides," *Chemical reviews*, 2001, 101: 1981.
- [5] T. Ishihara, *Perovskite oxide for solid oxide fuel cells*, vol. 16: Springer, 2009.
- [6] N. Mahato, A. Banerjee, A. Gupta, S. Omar, and K. Balani, "Progress in material selection for solid oxide fuel cell technology: A review," *Progress in Materials Science*, 2015, 72: 141.

- [7] J. Richter, P. Holtappels, T. Graule, T. Nakamura, and L. J. Gauckler, "Materials design for perovskite SOFC cathodes," *Monatshefte für Chemie-Chemical Monthly*, 2009, 140: 985.
- [8] N. Q. Minh, "Solid oxide fuel cell technology-features and applications," *Solid State Ionics*, 2004, 174: 271.
- [9] Y. Teraoka, H.-M. Zhuang, S. Furukawa, and N. Yamazoe, "Oxygen permeation through perovskite-type oxides," *Chemistry Letters*, 1985, 14: 1743.
- [10] S. Jiang, "A comparison of O₂ reduction reactions on porous (La,Sr)MnO₃ and (La,Sr)(Co,Fe)O₃ electrodes," *Solid State Ionics*, 2002, 146: 1.
- [11] R. A. Richardson, J. W. Cotton, and R. M. Ormerod, "Influence of synthesis route on the properties of doped lanthanum cobaltite and its performance as an electrochemical reactor for the partial oxidation of natural gas," *Dalton Transactions*, 2004, 19: 3110.
- [12] A. Dutta, J. Mukhopadhyay, and R. N. Basu, "Combustion synthesis and characterization of LSCF-based materials as cathode of intermediate temperature solid oxide fuel cells," *Journal of the European Ceramic Society*, 2009, 29: 2003.
- [13] L. Nie, Z. Liu, M. Liu, L. Yang, Y. Zhang, and M. Liu, "Enhanced Performance of La_{0.6}Sr_{0.4}Co_{0.2}Fe_{0.8}O_{3-δ} (LSCF) Cathodes with Graded Microstructure Fabricated by Tape Casting," *Journal of Electrochemical Science and Technology*, 2010, 1: 50.
- [14] Z. Junwu, S. Xiaojie, W. Yanping, W. Xin, Y. Xujie, and L. Lude, "Solution-Phase Synthesis and Characterization of Perovskite LaCoO₃ Nanocrystals via A Co-Precipitation Route," *Journal of Rare Earths*, 2007, 25: 601.
- [15] S. P. Jiang and S. H. Chan, "A review of anode materials development in solid oxide fuel cells," *Journal of Materials Science*, 2004, 39: 4405.
- [16] E. P. Murray, M. Sever, and S. Barnett, "Electrochemical performance of (La,Sr)(Co,Fe)O₃-(Ce,Gd)O₃ composite cathodes," *Solid State Ionics*, 2002, 148: 27.
- [17] K. T. Lee and E. D. Wachsman, "Role of nanostructures on SOFC performance at reduced temperatures," *MRS Bulletin*, 2014, 39: 783.
- [18] T. E. Burye and J. D. Nicholas, "Improving La_{0.6}Sr_{0.4}Co_{0.2}Fe_{0.8}O_{3-δ} infiltrated solid oxide fuel cell cathode performance through precursor solution desiccation," *Journal of Power Sources*, 2015, 276: 54.
- [19] Z. Duan, M. Yang, A. Yan, Z. Hou, Y. Dong, Y. Chong, et al., "Ba_{0.5}Sr_{0.5}Co_{0.8}Fe_{0.2}O_{3-δ} as a cathode for IT-SOFCs with a GDC interlayer," *Journal of power sources*, 2006, 160: 57.
- [20] A. Mai, V. A. Haanappel, F. Tietz, and D. Stöver, "Ferrite-based perovskites as cathode materials for anode-supported solid oxide fuel cells: part II. Influence of the CGO interlayer," *Solid State Ionics*, 2006, 177: 2103.
- [21] E. Mostafavi, A. Babaei, and A. Ataie, "Synthesis of Nano-Structured La_{0.6}Sr_{0.4}Co_{0.2}Fe_{0.8}O₃ Perovskite by Co-Precipitation Method," *Journal of Ultrafine Grained and Nanostructured Materials*, 2015, 48: 45.
- [22] A. Babaei, L. Zhang, E. Liu, and S. P. Jiang, "Performance and stability of La_{0.8}Sr_{0.2}MnO₃ cathode promoted with palladium based catalysts in solid oxide fuel cells," *Journal of Alloys and Compounds*, 2011, 509: 4781.
- [23] J. Chen, et al., "Palladium and ceria infiltrated La_{0.6}Sr_{0.4}Co_{0.2}Fe_{0.8}O_{3-δ} cathodes of solid oxide fuel cells," *Journal of Power Sources*, 2009, 194: 275.
- [24] <http://www.fuelcellmaterials.com/powders-and-pastes/cathodes/LSCF-P>.
- [25] M. Sahibzada, S. Benson, R. Rudkin, and J. Kilner, "Pd-promoted La_{0.6}Sr_{0.4}Co_{0.2}Fe_{0.8}O₃ cathodes," *Solid State Ionics*, 1998, 113: 285.
- [26] X. Lou, S. Wang, Z. Liu, L. Yang, and M. Liu,

“Improving $\text{La}_{0.6}\text{Sr}_{0.4}\text{Co}_{0.2}\text{Fe}_{0.8}\text{O}_{3-\delta}$ cathode performance by infiltration of a $\text{Sm}_{0.5}\text{Sr}_{0.5}\text{CoO}_{3-\delta}$ coating,” *Solid State Ionics*, 2009, 180: 1285.